Applied Catalysis B: Environmental 176–177 (2015) 173–182

Contents lists available at ScienceDirect

Applied Catalysis B: Environmental

journal homepage: www.elsevier.com/locate/apcatb

Photocatalytic treatment of metoprolol with B-doped TiO_2: Effect of water matrix, toxicological evaluation and identification of intermediates

Rodrigo Pereira Cavalcante [a], Renato Falcao Dantas [b], Heberton Wender [c], Bernardí Bayarri [d], Oscar González [d], Jaime Giménez [d,*], Santiago Esplugas [d], Amilcar Machulek Jr. [a]

[a] Institute of Chemistry, Federal University of Mato Grosso do Sul, Av. Senador Filinto Muller, 1555, CP 549, CEP 79074-460 Campo Grande, MS, Brazil
[b] School of Technology, University of Campinas-UNICAMP, Paschoal Marmo 1888, Limeira, SP 13484-332, Brazil
[c] Institute of Physics, Federal University of Mato Grosso do Sul, Av. Senador Filinto Muller, 1555, CP 549, CEP 79070-900 Campo Grande, MS, Brazil
[d] Department of Chemical Engineering, University of Barcelona, C/ Martí i Franquès 1, 08028 Barcelona, Spain

ARTICLE INFO

Article history:
Received 5 February 2015
Received in revised form 27 March 2015
Accepted 3 April 2015
Available online 4 April 2015

Keywords:
Heterogeneous photocatalysis
TiO_2/5%B(w/w)
Drug metoprolol
Effluent organic matter
Biodegradability

ABSTRACT

The aim of this study was to investigate the effectiveness of B doped TiO_2 on the removal of metoprolol tartrate salt (MET) in ultrapure water (UW) and municipal secondary effluent (SE) using a Xenon lamp (photon flux of 2.99×10^{-6} Einstein s^{-1}) as irradiation source. The analyzed parameters were MET removal, total organic carbon (TOC), chemical oxygen demand (COD), biochemical oxygen demand (BOD_5) and acute toxicity (Microtox®). The optimal photocatalyst concentration was determined in both matrices. After 180 min of irradiation, 70% and 44% of MET were removed using 0.4 g L^{-1} catalyst in UW and 2.0 g L^{-1} catalyst in SE, respectively. A substantial improvement of biodegradability (BOD_5/COD) was also achieved. The acute eco-toxicity decreased when MET was degraded and no toxic products were formed at the end of the process. Several reaction intermediates generated during the MET removal were identified and a possible degradation pathway was proposed for the TiO_2/5%B(w/w) reaction. Photocatalysis with B-doped TiO_2 can be considered as an interesting MET degradation alternative, leading to higher removals and potential to use solar energy, thus, minimizing the operating costs.

1. Introduction

Pharmaceuticals on environmental samples are considered to present a potential risk for aquatic and terrestrial organisms [1,2]. These drugs enter the water bodies through various sources, such as direct disposal of drugs surplus in households, excretion by humans and animals, and inadequate treatment of manufacturing effluents [3]. Treatability studies demonstrate that some of these drugs are not completely removed through conventional urban wastewater treatment plants and, as a result, they are introduced into the aquatic environment at concentration ranging from ng L^{-1} to μg L^{-1} [1,4]. Therefore, they are assumed to be environmentally relevant pollutants [2,5,6].

Among the large number of drugs that can be detected in effluents, β-blockers are considered emerging contaminants because they are widely used, not only in hospitals but also in household in daily treatment of patients. As a consequence, its occurrence in aqueous effluents is expected to increase [7]. Metoprolol and atenolol are indeed among the 20 most commonly encountered pharmaceuticals in European waters [8,9]. These drugs, together, account for more than 80% of total β-blockers consumption in Europe [10].

Metoprolol tartrate salt (MET {1-[4-(2-methoxyethyl) phenoxy]-3-(propan-2-ylamino)propan-2-ol tartrate (2:1)}) is one of the most common β-blocker. It is used for the treatment of different cardiovascular diseases, such as hypertension, coronary artery disease and arrhythmias [7,11,12]. This β-blocker has been detected in the order of ng L^{-1}–μ g L^{-1} in the surface waters [13–15].

The use of advanced oxidation processes (AOPs) as pretreatment for improving the biodegradability and efficacy of further treatments is recommended for effluents that contain high concentrations of recalcitrant pollutants, including pharmaceuticals [1,16–21]. These methods rely on the formation of highly

* Corresponding author. Tel.: +34 934021293.
E-mail address: j.gimenez.fa@ub.edu (J. Giménez).

http://dx.doi.org/10.1016/j.apcatb.2015.04.007
0926-3373/

reactive chemical species which degrade even the most recalcitrant molecules into biodegradable compounds [22]. Although the strong potential of AOPs for wastewater treatment is widely recognized, it is also well known that the operating costs for total oxidation of hazardous organic compounds remain relatively high compared to those of biological treatment. However, the total destruction of contaminants is not always necessary [23]. While AOP operating costs are always higher than those of a biological treatment, their use as a pre-treatment for the enhancement of the biodegradability of wastewater containing recalcitrant or treatment-inhibiting compounds might be justified. The intermediate reaction products could then be degraded by microorganisms in a biological post-treatment [23].

Among the different AOPs, heterogenous photocatalysis based upon TiO_2 can be an interesting option. TiO_2 is considered as the best known semiconductor for photocatalysis due to its good efficiency and stability, low cost, and possibility of activation by sunlight. Furthermore, it is non-specific and can degrade successfully a large variety of toxic compounds [2,15,24,25].

Many researchers have highlighted many advantageous sides of photocatalysis in presence of TiO_2 nanoparticles. However, as any technology, there are still several numerous drawbacks associated to the use of TiO_2. The scale up of heterogeneous photocatalysis process is the main challenging task [26]. In addition, the photocatalytic activity of TiO_2 is limited by the low interfacial charge-transfer rates of photogenerated carriers as well as its high charge carriers recombination rate [27]. The recovery and reuse of TiO_2 nanoparticles at the end of photocatalysis process are other drawbacks and very tedious jobs in practice [26]. Another significant problem is given by the "shadowing effect" that the suspension of the photocatalyst exerts against the radiation that activates the process itself ultimately resulting in reduced irradiation intensity [28]. Thus, photocatalysis application in full scale water treatment is still difficult because of the low efficiency of photocatalysis when compared to other treatment techniques. However, for certain applications the photocatalysis can be very useful. An example is the plant for the treatment of washing waters of pesticide containers, located in Almeria (Spain). Another example is the photocatalysis application in disinfection of water in third world areas, etc. It is therefore, appropriate further investigate this technology to be extending its scope.

Due TiO_2 to be considered one of the best semiconductor for photocatalysis has also led to the development of several preparation methods, including TiO_2 in the form of powder, crystals or thin films. Among the various synthesis methods, the sol–gel method provides synthesis of nanoparticles at ambient temperature and atmospheric pressure. Since this process occurs in a solution, many advantages over other manufacturing techniques can be cited, among them: the obtaining of materials with high purity, simplicity, ease and flexibility in introduction of dopants in large concentrations and homogeneity [29–32].

Doping of TiO_2 with non-metals, such as nitrogen, fluorine, sulfur and boron, allows improving the photocatalytic reactivity of TiO_2 [32]. At the best of our knowledge, MET photocatalytic studies have been reported [11,12,15,29–31,33–36], but none of them have employed doped TiO_2 and only three works involve the preparation of TiO_2 by sol–gel method [29–31].

In a previous work [37], we studied the preparation and evaluation of new photocatalysts based on TiO_2 doped with Boron by sol–gel technique in different proportions of boron (0–9% w/w). The photocatalytic activity of the catalysts was evaluated by the photodegradation of MET in deionized water. Results showed that the 5% w/w B-doped TiO_2 exhibited greater photodegradation (70% MET removal) than pure TiO_2 (48% MET removal). The results indicated that the physical and chemical changes introduced in the catalyst particles after the doping (increased surface area, formation of mesoporous structure, uniformity in particles surface size, formation of double-phase structure of anatase and rutile, decrease of TiO_2 crystal and particle size) were responsible for the photocatalytic performance of 5% B-doped TiO_2. According to the literature [38–40] other factors could be responsible for that improvement in the performance, such as a lower e^-/h^+ recombination; formation of two new chemical bonds with a doping B—O—Ti and B—O—B, which benefit photodegradation; formation of Ti(III), which reduces the recombination of photoexcited electrons and holes; expansion of the visible region radiation absorption. However, contrary to the literature data, the obtained B-TiO_2 did not result in the improvement of TiO_2 photocatalytic efficiency in visible light range, proved by the E_{gap} measurements. The goal of this work is to evaluate the effect of the 5% w/w B-doped TiO_2 catalyst concentration and the effect of the water matrix (i.e., pure water and secondary effluent) used for the preparation of MET solution. For the optimal conditions in both matrices, the mineralization, oxidation, biodegradability and acute toxicity using Microtox® test were investigated. Additionally, an attempt has been completed to identify the intermediates formed during the photocatalytic degradation.

2. Materials and methods

2.1. Chemicals

All chemicals were of analytical grade. Metoprolol tartrate salt (MET, purity >99%) (CAS n° 56392-17-7/$(C_{15}H_{25}NO_3)_2C_4H_6O_6$, MW 684.81 g mol^{-1}) was purchased from Sigma–Aldrich Chemical Co. Acetonitrile, used as mobile phase for HPLC, was purchased from Fisher Chemical. Other chemicals and solvents were purchased from various commercial suppliers and used as received. The used filters were Millipore Millex syringe-driven 0.45-μm (pore size) polyethersulfone membrane filters.

2.2. Effluent sample and characterization

MET solutions (50 mg L^{-1}) were prepared in ultrapure water (UW) and municipal secondary effluent (SE). SE was collected from the secondary biological treatment effluent of the municipal wastewater treatment plant (MWTP) located in Gavà-Viladecans (Barcelona, Spain). The MWTP serves a population of 300,000 equivalent inhabitants and uses the conventional activated sludge processes. After collection, samples were transported to the laboratory and stored at 4 °C. The effluent was filtered using 10 μm filter before analysis and experimentation. Its physicochemical characterization is described in Table 1. For the experiments of BOD_5 and acute ecotoxicity the pH of the samples was adjusted with NaOH and H_2SO_4 solutions.

2.3. B-TiO_2 photocatalyst preparation

Boron-modified TiO_2 (5% w/w of B) catalyst was prepared following a simple modified sol–gel method [41,42] using titanium tetra-isopropoxide as TiO_2 precursor and boric acid as boron precursor. The procedure consists in mixing titanium(IV) isopropoxide with glacial acetic acid (molar ratio H^+/Ti 1:4), under constant stirring, to form the complex. The acetic acid acted as chelating agent to control the hydrolysis process. Thus, the solution was diluted with 2-propanol at 1:1 (v/v) Ti/alcohol ratio and stirred for 1 h. In the following step, 1.44 g of H_3BO_3 were dissolved in a solution containing water and nitric acid, then this solution was added to the mixture under continuous stirring, keeping the molar ratios at H_2O/Ti = 25 and H^+/Ti = 0.5. The solution was stirred for 2 h and subsequently kept at 40 °C for around 48 h. The resulting TiO_2-

Table 1
Physicochemical parameters of SE.

Parameter	Value
TOC (mg C L^{-1})	18.8
UV_{254} (cm^{-1})	0.235
COD (mg O_2 L^{-1})	44.6
BOD_5 (mg O_2 L^{-1})	8.4
pH	7.56
Turbidity (NTU)	10.4
Alkalinity (mg $CaCO_3$ L^{-1})	471
Total suspended solids, TSS (mg L^{-1})	18.8
Volatile suspended solids, VSS (mg L^{-1})	14.6
Cl^- (mg L^{-1})	745
Br^- (mg L^{-1})	0.0
NO_3^- (mg L^{-1})	3.0
NO_2^- (mg L^{-1})	0.0
F^- (mg L^{-1})	0.0
PO_4^{3-} (mg L^{-1})	15
SO_4^{2-} (mg L^{-1})	232
NH_4^+ (mg L^{-1})	57.1
Na^+ (mg L^{-1})	495
K^+ (mg L^{-1})	45.9
Ca^{2+} (mg L^{-1})	138
Mg^{2+} (mg L^{-1})	59.6

B solution was dried in an oven at 100 °C for 24 h. The obtained powder was macerated in a mortar and calcined at 450 °C for 4 h.

2.4. Structural characterization of B-TiO_2 by X-ray diffraction (XRD) and Rietveld refinements

X-ray powder diffraction (XRD) analysis were performed in a PANalytical X'Pert PRO MPD Alpha1 powder diffractometer, in Bragg–Brentano $\theta/2\theta$ geometry from 4° to 100° (2θ) by using Cu Kα (λ = 1.542 Å) radiation. Intensity measurements were conducted with step sizes of 0.017° with 50 s of measuring time per step. Rietveld refinements [43] were calculated using the package General Structure Analysis System (GSAS) program [44], and graphical user interface EXPGUI [45]. Peak profile functions were modeled using a convolution of the Thompson–Cox–Hastings pseudo-Voigt function and, to account axial divergence, the asymmetry function described by Finger et al. [46]. To discount instrumental broadening of the diffraction peaks, LaB_6 NIST SRM-660a was measured using $\theta/2\theta$ scan from 20 to 152° with step size of 0.008° with measuring time of 384 s per step. The instrumental parameters obtained by refining this standard sample was used as input for the refinement of the TiO_2 + 5% w/w of B sample prepared in this work.

2.5. Experimental set up

Photocatalysis experiments were carried out in a solar simulator (Solarbox, Co.fo.me.gra, 220 V, 50 Hz, see Fig. 1) equipped with a Xenon lamp (Phillips XOP 1 kW) and an optical filter (cut-off <280 nm) located just below the lamp. The photon flux was 2.99×10^{-6} Einstein s^{-1} (290–400 nm), determined by *o*-nitrobenzaldehyde (*o*-NB) actinometry [47]. The MET aqueous solution (50 mg L^{-1}) was placed in a stirred reservoir tank (1.0 L). Thus, the aqueous suspension was continuously pumped (peristaltic pump Ecoline VC-280 II, Ismatec) into a Duran tubular photoreactor (24 cm length, 2.11 cm diameter, 0.078 L illuminated volume) placed at the bottom of the solarbox in the axis of a parabolic mirror. The solution was recirculated to the reservoir tank at a flow rate of 0.65 L min^{-1}. In order to keep the solution at 25 °C, the jacket temperature of the stirred tank was controlled with a thermostatic bath (Haake K10).

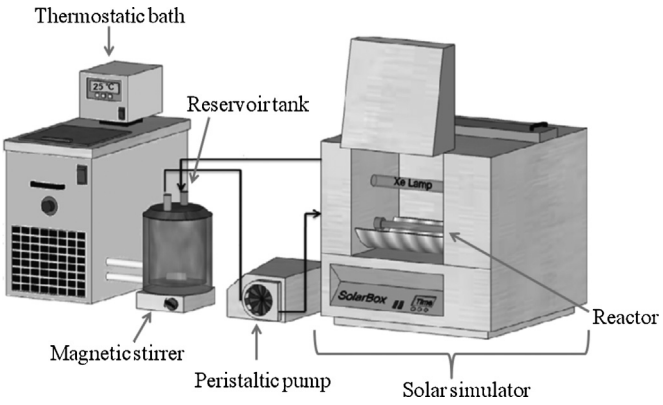

Fig. 1. Solar simulator and experimental device.
Source: Adapted from Romero et al. [36].

2.6. Analytical procedures

MET degradation was monitored by a high-performance liquid chromatography (HPLC) 1200 Infinity Series from Agilent under the following conditions: C18 reverse phase column (SEA18 5 μm 15 × 0.46 cm from Teknokroma), water and acetonitrile (78:22) as the mobile phase, injected with a flow-rate of 0.850 mL min^{-1}, and a Waters 996 photodiode array detector using the Empower Pro software 2002 Water Co., working at maximum UV absorbance in 221.9 nm. In order to remove the catalyst, before the analysis, samples were filtered with a polyethersulfone membrane filter of 0.45 μm.

TOC was measured using a Shimadzu TOC-VCNS instrument. To analyze the COD, colorimetric method 5220D [48] of Standard Methods procedures was followed by use of a spectrophotomer (Hach Lange DR 2500) at 420 nm, employing Pyrex-glass vials, after 2 h of extreme catalytic oxidation conditions at 150 °C. BOD_5 determinations were carried out according to the Standard Methods 5210D procedures [48] using the WTW OxiTop measuring system (Weilheim, Germany), thermostated at 20 °C.

The acute ecotoxicity of the samples was measured by the Microtox® test, in which the inhibition of *Vibrio fischeri* bioluminescence at 15 min of incubation was determined. Results obtained in this test can be expressed as $EC_{50,15\,min}$. It represents the percentage (%v/v) of the initial solution that causes a 50% of bioluminescence reduction in 15 min of contact. It can also be expressed as the inverse of this percentage in the form of toxicity units, $TU = 100/EC_{50}$.

For the intermediates identification, samples were analyzed by using an HPLC system (Agilent Series 1100, Agilent Technologies) under the same conditions used previously for monitoring degradation of MET. The HPLC system is connected to LC/MSD-TOF (Agilent Technologies) mass spectrometer operated in the positive electrospray ionization mode (ESI–MS) and using the following parameters: capillary 4000 V; nebulizer 15 psig; drying gas 7 L min^{-1}; gas temperature 325 °C; fragmentator 175 V. Spectra were acquired over the *m*/*z* 60–1200 range.

3. Results and discussion

3.1. Characterization results of B/TiO_2 catalyst

The catalysts used in this work (TiO_2/B(5%w/w)) were characterized in a previous study [37]. The main results of characterization were: specific surface area 100 m^2 g^{-1}; size of the particle 10.54 nm; bandgap energy (E_{bg}) value 3.04 eV; size of pore diameter 8.49 nm; atomic percentage of boron 17.8% and pH_{zpc} (pH at point of zero charge) of catalyst 5.34.

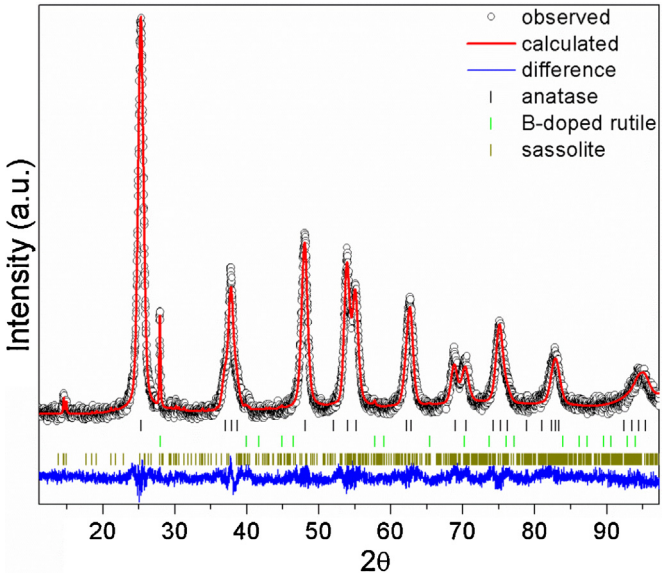

Fig. 2. Rietveld plot of TiO_2/B(5% w/w). The reduced chi^2, WRp and Rp parameters of the fit are 1.631, 0.0830 and 0.0636, respectively. The calculated and observed patterns are presented, respectively, as red line and black circles with residue as blue line. (For interpretation of the references to color in this figure legend, the reader is referred to the web version of this article.)

Rietveld refinements were performed to extend the characterization of B-doped TiO_2 nanocrystals in order to understand the hole of B insertion into TiO_2 structure. The sample analyzed was TiO2/B(5%w/w). Almost all peaks from the diffractogram could be indexed for TiO_2 anatase crystalline phase as also observed in the undoped sample prepared in our previous work [37]. However, two small peaks near 2θ of 15° and an intense and relatively fine peak at 27.8° were additionally detected. Fig. 2 shows the Rietveld plot of the final fitting that only converged when performed considering 3 crystalline phases, namely, TiO_2 anatase (CIF Code 96946), B-doped rutile TiO_2 (CIF code 82657) and H_3BO_3 (CIF code 24711) that could be formed through B_2O_3 and subsequent adsorption of water molecules, as described elsewhere [49]. As it can be seen, the results indicate that boron was incorporated into the rutile phase [50]. The quantitative phase analysis resulted in 94.4% of anatase, 0.7% of B-doped rutile and 4.9% of sassolite H_3BO_3 phase. The refined unitary cell parameters are available in Table S1 of Supplementary material.

3.2. Influence of B/TiO_2 concentration and matrix on MET removal

The determination of the optimal concentration of TiO_2/B(5%w/w) was performed on two types of matrices: UW and SE to assess the influence of organic matter present in the SE. Several authors have investigated the reaction efficiency as a function of catalyst concentration in photocatalytic process [36,51–55]. Fig. 3 (A and B) shows the degradation of MET at different concentrations of catalyst. TiO_2/B(5%w/w) concentration ranged from 0.2 to 1.5 g L^{-1} and from 0.4 to 2.5 g L^{-1} in the experiments with UW and SE, respectively. The range of catalyst concentrations was different on both matrices because organic matter present in the SE inhibits the degradation of MET and a greater amount of catalyst is needed to achieve higher conversions of the target compound [51].

The optimal catalyst concentration was 0.4 g L^{-1} for the MET removal in UW experiments (70% removal of MET) (Fig. 3A). There was no significant improvement in MET removal for catalyst concentrations higher than 0.4 g L^{-1}.

Similar results have been reported in previous studies [51]. According to Ghaly et al. [51], this fact can be due to the increase in aggregates formation, causing a decrease in the number of active surface sites. Higher concentrations of TiO_2 can also imply an increasing opacity of solution which leads to a decrease in the radiation passing through the sample, and therefore, a part of the catalyst surface becomes unavailable for photon absorption, and degradation rate decreases. Related to all this, light scattering can increase and the efficiency can be reduced. The decrease of the degradation rate at higher catalyst concentrations may also be due to deactivation of activated molecules by collision with ground state molecules. The shielding of TiO_2 (Eq. (1)) may also occur [51].

Table 2
Kinetic constant (k_{ap}) values for MET removal using TiO_2-doped with 5% B.

Matrices	Catalyst concentration (g L^{-1})	k_{ap} (min^{-1})	R
UW	0.4	7.05×10^{-3}	0.995
	0.6	5.34×10^{-3}	0.997
	1.0	6.38×10^{-3}	0.993
	1.5	6.47×10^{-3}	0.996
SE	0.4	9.72×10^{-4}	0.999
	1.0	1.97×10^{-3}	0.999
	1.25	2.05×10^{-3}	0.997
	1.5	2.20×10^{-3}	0.999
	2.0	3.29×10^{-3}	0.997
	2.5	2.31×10^{-3}	0.999

$$TiO_2^* + TiO_2 \rightarrow TiO_2 + TiO_2^{\#} \quad (1)$$

TiO_2^* is the TiO_2 with active species adsorbed on its surface and $TiO_2^{\#}$ the deactivated form of TiO_2.

A different behavior was observed in the experiments with MET prepared in SE (Fig. 3B). The results clearly show that the increase of catalyst concentration from 0.4 to 2.0 g L^{-1} improves the MET removal (45%). In this case, there is a competition for the surface of titania between the MET and the organic matter (see Table 1) present in the SE. In addition, a competition for UV absorption might not be neglected. For these reasons, a higher catalyst concentration seems to be needed to achieve higher MET conversions [51]. The organic matter from SE competes for active species generated in the process and also adsorbs in the photocatalyst surface, inhibiting the MET degradation. The possible interference of inorganic ions, which can cause deactivation of the catalyst surface [55], should also be considered.

In order to compare the MET removal rate in the different experimental conditions, the pseudo-first order kinetic constant (k_{ap}) was calculated for each concentration of catalyst in both matrices (see Table 2). k_{ap} values could be obtained from the regression line slopes representing $-\ln(C/C_o)$ vs. time. These results corroborate that the best catalyst concentration for removal of MET was 0.4 g L^{-1} in UW and 2.0 g L^{-1} in SE. In addition, k_{ap} values for SE matrix are lower than these ones for UW matrix, indicating the influence of organic matter and/or inorganic ions, present in SE, for the MET removal.

Once the best concentration of titania to remove MET in both matrices was determined, organic matter oxidation, mineralization, biodegradability and toxicity removal were studied.

3.2.1. Mineralization and oxidation removal

Fig. 4A and B shows the normalized TOC and COD removal during the photocatalytic treatment with the optimal concentrations of catalysts.

In the experiments in UW (Fig. 4A), COD and TOC removals decreased significantly during the irradiation time, achieving values near 32 and 25%, respectively, after 180 min of treatment.

In experiments using SE (Fig. 4B), 35% of COD removal was obtained. However, the resultant mineralization was lower (12%), this shows that the compounds present in the effluent are resistant to mineralization. The initial values of COD and TOC for MET

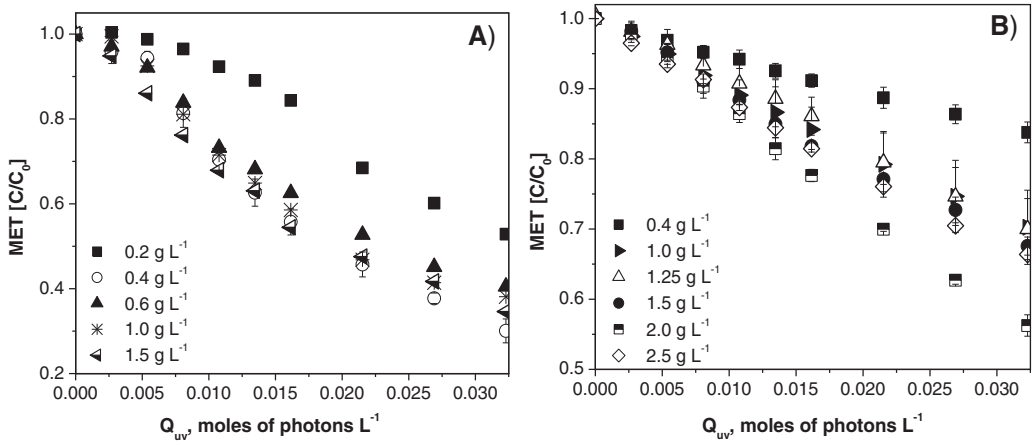

Fig. 3. Effect of the B/TiO_2 concentration on MET degradation with solutions (50 mg L^{-1} MET) prepared in (A) UW and (B) SE.

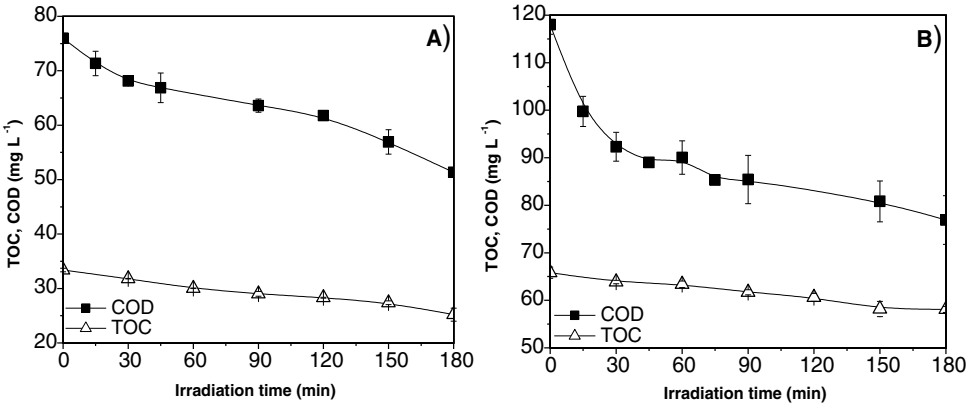

Fig. 4. Oxidation (COD) and mineralization (TOC) for MET photocatalysis, using (A) 0.4 g L^{-1} of TiO_2/B(5%w/w) in MET prepared with UW and (B) 2.0 g L^{-1} of TiO_2/B(5%w/w) in MET prepared with SE.

prepared in SE are around 120 and 65 mg L^{-1}, respectively, much higher than the COD and TOC values (44.6 and 18.8 mg L^{-1}, respectively) for MET prepared in UW. This demonstrates the high amount of organic matter present in SE and, consequently, the optimal amount of catalyst needed in SE was 5 times higher than in UW. These results clearly show that the spiked SE is susceptible to oxidation; nevertheless, it is very resistant to mineralization by photocatalysis using the studied catalyst.

3.2.2. Biodegradability and toxicity assessment

In order to better evaluate the suitability of the photocatalytic treatment for waters containing MET, the biodegradability and toxicity were measured. These are important parameters in case this process would come a pre-treatment for the enhancement of the biodegradability of wastewater containing recalcitrant, as a strategy to reduce overall operation costs [23,55].

The biodegradability was measured as BOD_5/COD. The experimental results (Fig. 5) showed that the biodegradability was improved by the tested photocatalytic oxidation. Before treatment, the value of biodegradability was low (MET + SE = 0.15 and MET + UW = 0.04). This means that the compounds solution before treatment is non-biodegradable. The biodegradability indicator increased and followed the same trend in both matrix with a final value of BOD_5/COD around 0.55. This value is higher than the reference value of 0.4, from which the solution can be considered readily biodegradable [55,56].

For additional information on the danger of discarding water containing MET and to verify the efficiency of photocatalysis, an

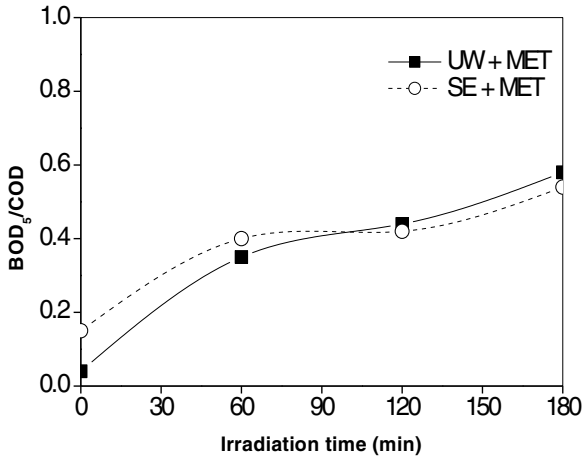

Fig. 5. Biodegradability promoted by B doped TiO_2 photocatalysis.

acute toxicity assessment (Microtox®) was also carried out. The results expressed in Equitox/m^3 are presented in Fig. 6. The oxidation of MET promoted the overall toxicity reduction of the sample since the beginning of the treatment in both matrices and no toxic product was generated at the end of the process, confirming the high potential applicability of the catalyst of TiO_2 doped with 5% (w/w) B for the removal of the MET.

During the photocatalytic process, MET suffers a progressive degradation with time of reaction. Regarding the degradation time,

Table 3
Intermediates identified for the photocatalytic degradation of MET by 5% B doped TiO_2.

Compound	Accurate mass of $[M+H]^+$	Mass accuracy (ppm)	(Retention time, min)	Molecular formula	Proposed structure
CP-268	268.20	<0.60	4.284	$C_{15}H_{25}NO_3$	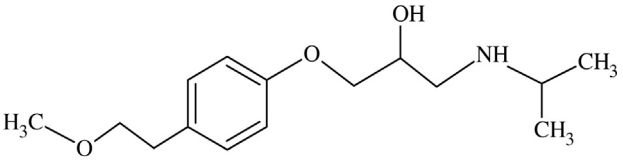 MET
CP-116	116.11	<2.00	2.33	$C_6H_{13}NO$	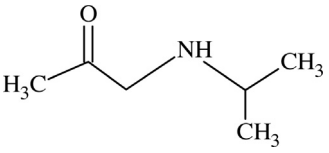
CP-120	120.10	<2.00	2.33	$C_5H_{13}NO_2$	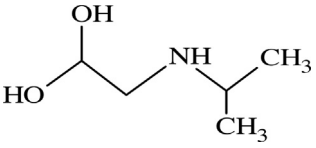
CP-134	134.12	<2.00	2.33	$C_6H_{15}NO_2$	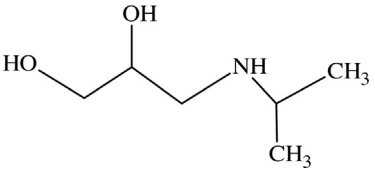
CP-150	150.11	<2.00	2.33	$C_6H_{15}NO_3$	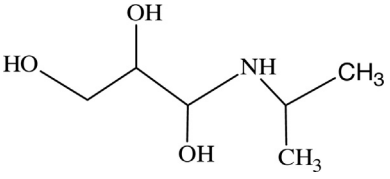
CP-226	226.14	<3.50	2.61	$C_{12}H_{19}NO_3$	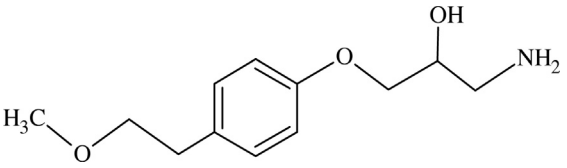
CP-238	238.14	<1.50	2.97	$C_{13}H_{19}NO_3$	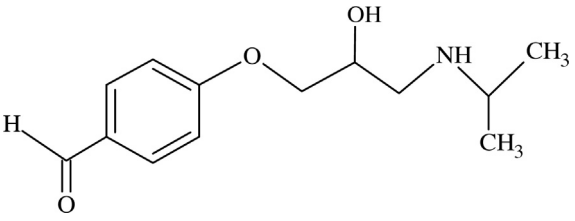
CP-240	240.16	<3.50	2.61	$C_{13}H_{21}NO_3$	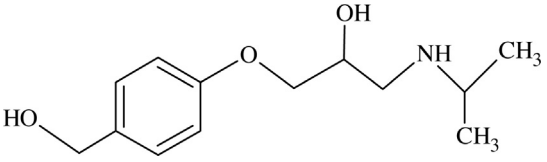
CP-252	252.16	<4.50	2.80	$C_{14}H_{21}NO_3$	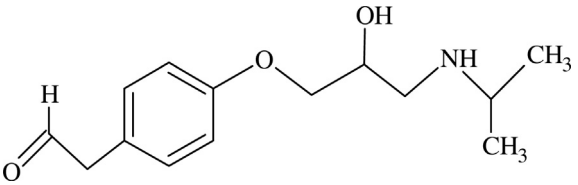

Table 3 (*Continued*)

Compound	Accurate mass of $[M+H]^+$	Mass accuracy (ppm)	(Retention time, min)	Molecular formula	Proposed structure
CP-254	254.17	<4.50	2.80	$C_{14}H_{23}NO_3$	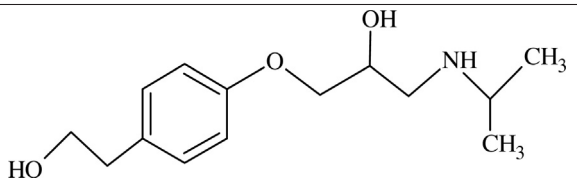
CP-256	256.16	<4.50	2.80	$C_{13}H_{21}NO_4$	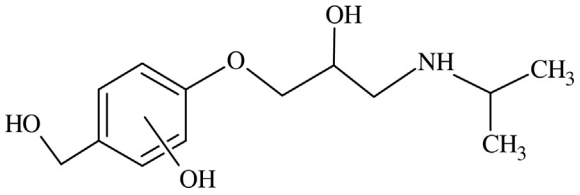
CP-270	270.16	<3.50	2.61	$C_{14}H_{23}NO_4$	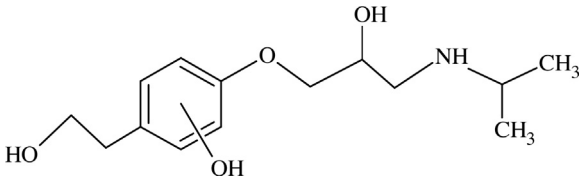
CP-282	282.17	<1.77	2.85	$C_{15}H_{23}NO_4$	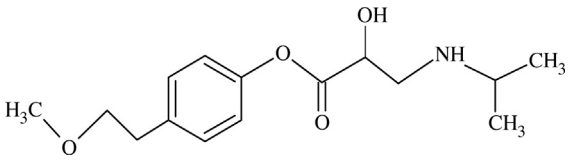
CP-284	284.19	<1.00	3.41	$C_{15}H_{25}NO_4$	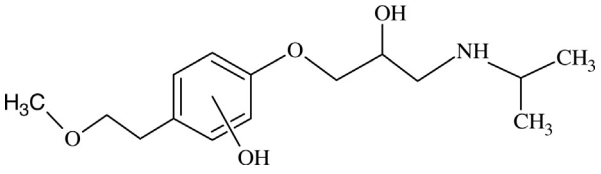
CP-298	298.17	<1.00	3.41	$C_{15}H_{23}NO_5$	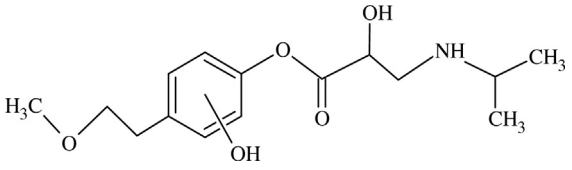
CP-300	300.18	<1.77	2.85	$C_{15}H_{25}NO_5$	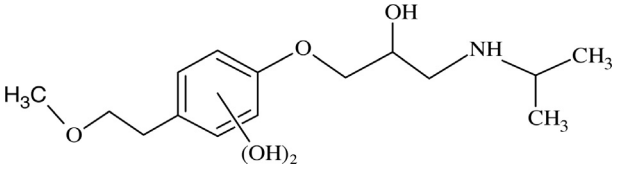
CP-316	316.18	<1.77	2.85	$C_{15}H_{25}NO_6$	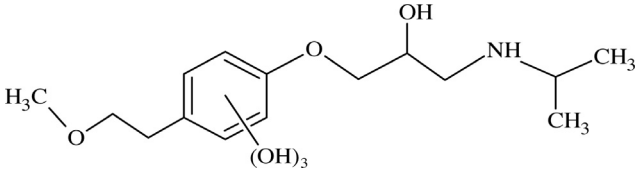
CP-318	318.19	<3.50	2.61	$C_{15}H_{27}NO_6$	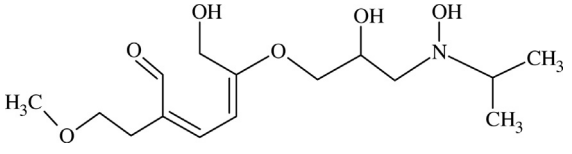

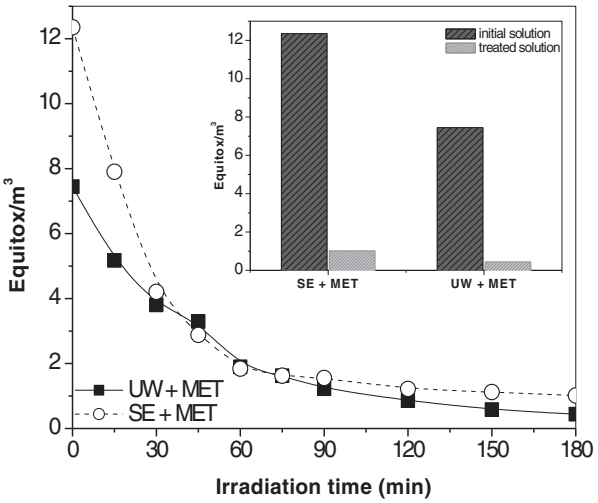

Fig. 6. Equitox for MET promoted by B doped TiO_2 reaction.

we use 180 min of photocatalytic treatment. The experimental results showed that the photocatalytic treatment increases the biodegradability (see Fig. 5) and reduces the overall toxicity since the beginning of the treatment, and no toxic products appear at the end of the process (see Fig. 6). Thus, high final degradation is not necessary, if products and subproducts formed are biodegradable and non-toxic. The minimum necessary time to pre-treatment the contaminated water can be optimized in order to stop the photochemical oxidation and reduce costs of operation. For this reason, we have not extended the degradation time.

3.3. Intermediates during reaction and degradation pathways

The photocatalytic degradation of MET occurs with the formation of different reaction intermediates. For the identification of by-products of MET degradation (experiment with 50 mg L^{-1} MET in UW, 0.4 g L^{-1} TiO_2 doped with 5% B), a sample mixture at 90 min and a final sample mixture at 180 min, were analyzed by electrospray ionization/mass spectrometry in positive electrospray. The masses of the different products were determined from the peaks corresponding to the protonated molecule, $[M+H]^+$. Fig. S1 (Supplementary material) shows the mass spectrum of MET and its intermediates. A total of 17 products of MET degradation at *m/z* 116, *m/z* 120, *m/z* 134, *m/z* 150, *m/z* 226, *m/z* 238, *m/z* 240, *m/z* 252, *m/z* 254, *m/z* 256, *m/z* 270, *m/z* 282, *m/z* 284, *m/z* 298, *m/z* 300, *m/z* 316 and *m/z* 318 were detected.

Table 3 shows the intermediates detected along the reaction time with the empirical formula obtained by the equipment software used (LC/MSD TOF ESI-TOF) and the probable molecular structures. Since the collision-induced dissociation patterns of MET degradation intermediates are well defined [57], it was possible to identify with confidence their intermediaries using LC–MS/TOF analysis.

The MET ($C_{15}H_{25}NO_3$) has a molecular weight $[M+H]^+ = 268$. Hydroxylated intermediates corresponding to the binding of HO• radicals in the aromatic ring were detected: monohydroxylated derivative of MET, different fragments of the monohydroxylated with *m/z* = 284, 270 and 256, dihydroxylated intermediates with *m/z* = 300 and trihydroxylated intermediates with *m/z* = 316. Similarly, the hidroxylated intermediates were also identified by other researchers [11,15,35,36,58–60]. On the other hand, Wilde et al. and Romero et al. identified an intermediate with *m/z* = 300 that would correspond to our trihydroxylated intermediates, but they proposed a different structure that involved the opening of the aromatic ring [7,12].

The attack of HO• on the C atom next to the ether functional group in the aliphatic part and the oxidation of the hydroxyl group of MET yields the keto-tautomer with *m/z* = 282. This intermediate was also identified by Abromovic et al., Romero et al. and Yu et al. [11,36,58]. Later the HO• attack on the C atoms of the aromatic ring of keto-tautomer yielded hydroxy intermediate with *m/z* = 298, as proposed by Abromovic et al. [11].

After the breaking of a C—C bond in the aliphatic part of the MET molecule, an amino-diol was identified with *m/z* = 134 which is a common degradation product of β-blockers by several different technologies as mentioned by many researchers [7,11,12,15,33,35,36,58–62]. Different intermediates of the ethanolamine side were also identified (*m/z* = 116, 120, 150), probably due to the loss of the hydroxyl group and the loss of isopropyl moiety and/or the oxidation of the hydroxyl group [15].

The peaks with *m/z* = 254, 252, 240 and 238, share the common fragmentation pattern and the formation of polar moieties (alcohols and aldehydes) probably by reactions which involve attack on the ether functional group of the MET molecule side chain followed by oxidation or elimination. These intermediates were reported by several researchers [7,33,36,59–61,63,64]. Abromovic

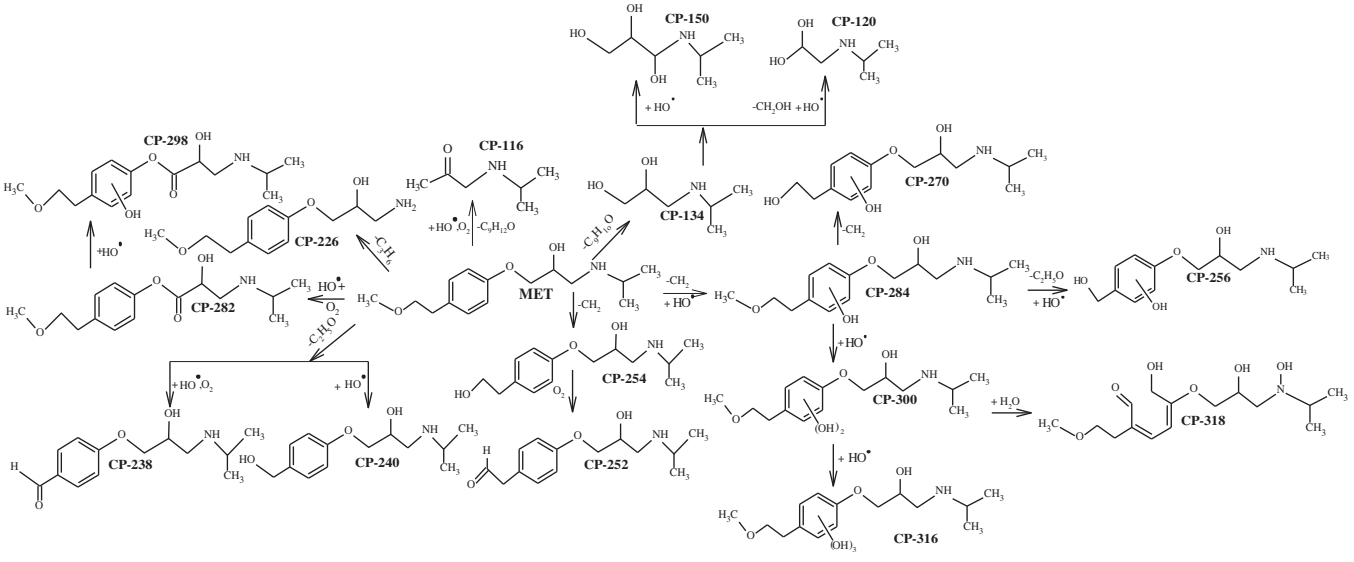

Fig. 7. Proposed MET degradation pathways for the main detected intermediaries by TiO_2/5%B(w/w) catalyst process.

et al. and Veloutsou et al. proposed different structures for these peaks [11,62].

Oxidative attack on the dimethylamine moiety results in cleavage and the formation of the intermediate with $m/z = 226$ [15,64]. The hydroxylation can leads to an opening of the aromatic ring. The intermediate with $m/z = 318$ shows the cleavage of the aromatic ring [12]. Although the intermediate with $m/z = 318$ would be formed due to an additional HO• attack on the amino group, this pathway of oxidation is not favored in the experimental conditions used because the process occurs at pH around 5.0 and the MET p*K*a is 9.6 and, consequently, the reactivity of the amino group is low. Probably, that occurs by a secondary reaction pathway [12]. At the best of our knowledge, intermediates with $m/z = 150$ and 156, as presented in this work, were not found in the literature.

According to all the mentioned in the previous paragraphs and by considering the identified intermediates (see Table 3), a possible degradation pathway for MET using TiO_2 doped with 5% B following different routes is shown in Fig. 7.

The reaction routes proposed in our work, although with some similarities, differ from others previously reported in the literature [11,15,36] for photocatalytic degradation process. MET follows similar, but not identical, reaction pathways in 5% B doped TiO_2 photocatalysis experiments. It is noteworthy that this is the first work that proposes a path of degradation using a catalyst synthesized by sol–gel method.

4. Conclusions

The photocatalytic treatment with TiO_2/5%B(w/w) has proved to be an effective method to remove MET in water. The organic matter present in real water (SE) strongly influences the degradation of the drug. A catalyst concentration five times higher (2.0 g L^{-1}) is needed to obtain a good performance in SE.

Photocatalytic oxidation of MET significantly increased biodegradability in both matrices (UW and SE). After degradation, the samples showed an overall toxicity reduction in comparison to the initial MET solution allowing safe disposal of the effluent. These factors encourage the use of the new synthesized photocatalysts as an effective technology for the treatment of MET.

The reaction of the main intermediates detected for the TiO_2/5%B(w/w) catalyst process were identified and a MET degradation pathway was proposed. The main pathways involved in the MET degradation are the hydroxylation of the benzene ring, shortening of methoxyl contained in the lateral chain, and cleavage or the addition of HO• to the amine lateral chain.

Acknowledgements

The authors wish to thank the Brazilian Funding Agencies CNPq (Conselho Nacional de Desenvolvimento Científico e Tecnológico), CAPES (Coordenação de Aperfeiçoamento de Pessoal de Nível Superior), FUNDECT (Fundação de Apoio ao Desenvolvimento do Ensino, Ciência e Tecnologia do Estado de Mato Grosso do Sul) and INCT-EMA (Instituto Nacional de Ciência e Tecnologia de Estudos do Meio Ambiente). The authors also thank the Ministry of Science and Innovation of Spain (projects CTQ2011-26258 and NOVEDAR 2010CSD2007-00055) and AGAUR – Generalitat de Catalunya (project 2009SGR 1466) for funds received to carry out this work.

Appendix A. Supplementary data

Supplementary data associated with this article can be found, in the online version, at http://dx.doi.org/10.1016/j.apcatb.2015.04.007.

References

[1] L.A. Ioannou, E. Hapeshi, M.I. Vasquez, D. Mantzavinos, D. Fatta-Kassinos, Sol. Energy 85 (2011) 1915–1926.
[2] M. Klavarioti, D. Mantzavinos, D. Kassinos, Environ. Int. 35 (2009) 402–417.
[3] L. Yang, L.E. Yu, M.B. Ray, Water Res. 42 (2008) 3480–3488.
[4] J. Choi, H. Lee, Y. Choi, S. Kim, S. Lee, S. Lee, W. Choi, J. Lee, Appl. Catal. B: Environ. 147 (2014) 8–16.
[5] K. Kümmerer, Chemosphere 75 (2009) 417–434.
[6] P. Verlicchi, A. Galletti, M. Petrovic, D. Barceló, J. Hydrol. 389 (2010) 416–428.
[7] M.L. Wilde, S. Montipó, A.F. Martins, Water Res. 48 (2014) 280–295.
[8] A. Rubirola, M. Llorca, S. Rodriguez-Mozaz, N. Casas, I. Rodriguez-Roda, D. Barceló, G. Buttiglieri, Water Res. 63 (2014) 21–32.
[9] S.R. Hughes, P. Kay, L.E. Brown, Environ. Sci. Technol. 47 (2013) 661–677.
[10] A.C. Alder, C. Schaffner, M. Majewsky, J. Klasmeier, K. Fenner, Water Res. 44 (2010) 936–948.
[11] B. Abramović, S. Kler, D. Sojić, M. Laušević, T. Radović, D. Vione, J. Hazard. Mater. 198 (2011) 123–132.
[12] V. Romero, N. De la Cruz, R.F. Dantas, P. Marco, J. Gimenez, S. Esplugas, Catal. Today 161 (2011) 115–120.
[13] M. Gros, M. Petrović, A. Ginebreda, D. Barceló, Environ. Int. 36 (2010) 15–26.
[14] M. Gros, M. Petrović, D. Barceló, Environ. Toxicol. Chem. 26 (2007) 1553–1562.
[15] V. Romero, P. Marco, J. Giménez, S. Esplugas, Int. J. Photoenergy (2013) http://dx.doi.org/10.1155/2013/138918
[16] F. Gozzi, A. Machulek Jr., V.S. Ferreira, M.E. Osugi, A.P.F. Santos, J.A. Nogueira, R.F. Dantas, S. Esplugas, S.C. Oliveira, Chem. Eng. J. 210 (2012) 444–450.
[17] A. De Luca, R.F. Dantas, A.S.M. Simões, I.A.S. Toscano, G. Lofrano, A. Cruz, S. Esplugas, Chem. Eng. Technol. 36 (2013) 2155–2162.
[18] A. Machulek Jr., J.E.F. Moraes, C. Vautier-Giongo, C.A. Silverio, L.C. Friedrich, C.A.O. Nascimento, M.C. Gonzalez, F.H. Quina, Environ. Sci. Technol. 41 (2007) 8459–8463.
[19] A. Machulek Jr., J.E.F. Moraes, C.A. Silverio, L.T. Okano, F.H. Quina, Photochem. Photobiol. Sci. 8 (2009) 985–991.
[20] F. Méndez-Arriaga, S. Esplugas, J. Giménez, Water Res. 44 (2010) 589–595.
[21] R.P. Cavalcante, L.R. Sandim, D. Bogo, A.M.J. Barbosa, M.E. Osugi, M. Blanco, S.C. Oliveira, M.F.C. Matos, A. Machulek Jr., V.S. Ferreira, Environ. Sci. Pollut. Res. 20 (2013) 2352–2361.
[22] S. Malato, P. Fernández-Ibáñez, M.I. Maldonado, J. Blanco, W. Gernjak, Catal. Today 147 (2009) 1–59.
[23] S. Malato, J. Blanco, A. Vidal, D. Alarcón, M.I. Maldonado, J. Cáceres, W. Gernjak, Sol. Energy 75 (2003) 329–336.
[24] L.M. Pastrana-Martínez, J.L. Faria, J.M. Doña-Rodríguez, C. Fernández-Rodríguez, A.M.T. Silva, Appl. Catal. B: Environ. 113–114 (2012) 221–227.
[25] D.D. Ramos, P.C.S. Bezerra, F.H. Quina, R.F. Dantas, G.A. Casagrande, S.C. Oliveira, M.R.S. Oliveira, L.C.S. Oliveira, V.S. Ferreira, S.L. Oliveira, A. Machulek Jr., Environ. Sci. Pollut. Res. 22 (2015) 774–783.
[26] S. Sarkar, S. Chakraborty, C. Bhattacharjee, Ecotoxicol. Environ. Saf. (2015), http://dx.doi.org/10.1016/j.ecoenv.2015.02.035.
[27] C.M. Teh, A.R. Mohamed, J. Alloy Compd. 509 (2011) 1648–1660.
[28] S. Murgolo, F. Petronella, R. Ciannarella, R. Comparelli, A. Agostiano, M.L. Curri, G. Mascolo, Catal. Today 240 (2015) 114–124.
[29] A. Golubović, B. Abramović, M. Šćepanović, M. Grujić-Brojčin, S. Armaković, I. Veljković, B. Babić, Z. Dohčević-Mitrović, Z.V. Popović, Mater. Res. Bull. 48 (2013) 1363–1371.
[30] M. Šćepanović, B. Abramović, A. Golubović, S. Kler, M. Grujić-Brojčin, Z. Dohčević-Mitrović, B. Babić, B. Matović, Z.V. Popović, J. Sol–Gel. Sci. Technol. 61 (2012) 390–402.
[31] M. Grujić-Brojčin, S. Armaković, N. Tomić, B. Abramović, A. Golubović, B. Stojadinović, A. Kremenović, B. Babić, Z. Dohčević-Mitrović, M. Šćepanović, Mater. Charact. 88 (2014) 30–41.
[32] U.G. Akpan, B.H. Hameed, Appl. Catal. A-Gen. 375 (2010) 1–11.
[33] V. Romero, O. González, B. Bayarri, P. Marco, J. Giménez, S. Esplugas, Catal. Today 240 (2015) 86–92.
[34] E. Moctezuma, E. Leyva, M. López, A. Pinedo, B. Zermeño, B. Serrano, Top. Catal. 56 (2013) 1875–1882.
[35] H. Yang, T. An, G. Li, W. Song, W.J. Cooper, H. Luo, X. Guo, J. Hazard. Mater. 179 (2010) 834–839.
[36] V. Romero, F. Méndez-Arriaga, P. Marco, J. Giménez, S. Esplugas, Chem. Eng. J. 254 (2014) 17–29.
[37] R.P. Cavalcante, R.F. Dantas, B. Bayarri, O. González, J. Giménez, S. Esplugas, A. Machulek Jr., Catal. Today (2014), http://dx.doi.org/10.1016/j.cattod.2014.09.030.
[38] L.G. Devi, R. Kavitha, Appl. Catal. B: Environ. 140–141 (2013) 559–587.
[39] S. Bagwasi, B. Tian, J. Zhang, M. Nasir, Chem. Eng. J. 217 (2013) 108–118.
[40] L. Liang, Y. Yulin, L. Xinrong, F. Ruiqing, S. Yan, L. Shuo, Z. Lingyun, F. Xiao, T. Pengxiao, X. Rui, Z. Wenzhi, W. Yazhen, M. Liqun, Appl. Surf. Sci. 265 (2013) 36–40.
[41] A.A. Cavalheiro, J.C. Bruno, M.J. Saeki, J.P.S. Valente, A.O. Florentino, Thin Solid Films 516 (2008) 6240–6244.
[42] S.M.A. Jorge, J.J. Sene, A.O. Florentino, J. Photochem. Photobiol. A: Chem. 174 (2005) 71–75.
[43] H.M. Rietveld, J. Appl. Cryst. 2 (1969) 65–71.
[44] A.C. Larson, R.B. Von Dreele, Los Alamos National Laboratory Report LAUR, 200486–748.

[45] B.H. Toby, J. Appl. Cryst. 34 (2001) 210–213.
[46] L.W. Finger, D.E. Cox, A.P. Jephcoat, J. Appl. Cryst. 27 (1994) 892–900.
[47] N. De la Cruz, V. Romero, R.F. Dantas, P. Marco, B. Bayarri, J. Giménez, S. Esplugas, Catal. Today 209 (2013) 209–214.
[48] Standard Methods for the Examination of Water and Wastewater, 21st ed., American Public Health Association/American Water Works Association/Water Pollution Control Federation, Washington, DC, USA (2005).
[49] O.M. Moon, B.-C. Kang, S.-B. Lee, J.-H. Boo, Thin Solid Films 464–465 (2004) 164–169.
[50] I.E. Grey, C. Li, C.M. MacRae, L.A. Bursill, J. Solid. State. Chem. 127 (1996) 240–247.
[51] M.Y. Ghaly, T.S. Jamil, I.E. El-Seesy, E.R. Souaya, R.A. Nasr, Chem. Eng. J. 168 (2011) 446–454.
[52] E.S. Elmolla, M. Chaudhuri, Desalination 252 (2010) 46–52.
[53] P.A. Pekakis, N.P. Xekoukoulotakis, D. Mantzavinos, Water Res. 40 (2006) 1276–1286.
[54] M.N. Abellán, J. Giménez, S. Esplugas, Catal. Today 144 (2009) 131–136.
[55] N. De la Cruz, R.F. Dantas, J. Giménez, S. Esplugas, Appl. Catal. B: Environ. 130–131 (2013) 249–256.
[56] Metcalf & Eddy Inc. Revised by G. Tchobanoglous, F.L., Burton, Wastewater Engineering, Treatment, Disposal and Reuse, third ed., McGraw-Hill, McGraw-Hill series in water resources and environmental engineering., New York (1991).
[57] R.M. Borkar, B. Raju, R. Srinivas, P. Patel, S.K. Shetty, Biomed. Chromatogr. 26 (2012) 720–736.
[58] Y. Yu, Y. Liu, X. Wu, Z. Weng, Y. Hou, L. Wu, Sep. Purif. Technol. 142 (2015) 1–7.
[59] D. Šojić, V. Despotović, D. Orčić, E. Szabó, E. Arany, S. Armaković, E. Illés, K. Gajda-Schrantz, A. Dombi, T. Alapi, E. Sajben-Nagy, A. Palágyi, L. Cs Vágvölgyi, Manczinger, L. Bjelica, B. Abramović, J. Hydrol. 472–473 (2012) 314–327.
[60] W. Song, W.J. Cooper, S.P. Mezyk, J. Greaves, B.M. Peake, Environ. Sci. Technol. 42 (2008) 1256–1261.
[61] J. Radjenovic, B.I. Escher, K. Rabaey, Water Res. 45 (2011) 3205–3214.
[62] S. Veloutsou, E. Bizani, K. Fytianos, Chemosphere 107 (2014) 180–186.
[63] J. Benner, T.A. Ternes, Environ. Sci. Technol. 43 (2009) 5472–5480.
[64] M.L. Wilde, W.M.M. Mahmoud, K. Kümmerer, A.F. Martins, Sci. Total Environ. 452–453 (2013) 137–147.